EFDA–JET–CP(14)01/07

L. Colas, Ph. Jacquet, D. Van Eester, V. Bobkov, M. Brix, L. Meneses, P. Tamain, S. Marsen, C. Silva, D. Carralero, M. Kocan, H.-W. Müllerd, K. Crombé, A. Krivska, M. Goniche, E. Lerche, F.G. Rimini, ASDEX-Upgrade team and JET EFDA contributors

Localized Scrape-Off Layer Density Modifications by Ion Cyclotron Near Fields in JET and ASDEX-Upgrade L-mode Plasmas

Localized Scrape-Off Layer Density Modifications by Ion Cyclotron Near Fields in JET and ASDEX-Upgrade L-mode Plasmas

L. Colas[1], Ph. Jacquet[2], D. Van Eester[3], V. Bobkov[4], M. Brix[2], L. Meneses[2], P. Tamain[1], S. Marsen[2], C. Silva[5], D. Carralero[4], M. Kocan[4,6], H.-W. Müllerd[4], K. Crombé[3], A. Krivska[3], M. Goniche[1], E. Lerche[3], F.G. Rimini[2], ASDEX-Upgrade team and JET EFDA contributors*

JET-EFDA, Culham Science Centre, OX14 3DB, Abingdon, UK

[1]CEA, IRFM, F-13108 Saint-Paul-Lez-Durance, France
[2]EURATOM-CCFE Fusion Association, Culham Science Centre, OX14 3DB, Abingdon, OXON, UK
[3]LPP-ERM-KMS, TEC partner, Brussels, Belgium
[4]Max-Planck-Institut für Plasmaphysik, Garching, Germany
[5]Instituto de Plasmas e Fusão Nuclear, Instituto Superior Técnico, Universidade de Lisboa, Portugal
[6]ITER Organization, Route de Vinon-sur-Verdon, CS 90 046, F-13067 St Paul lez Durance Cedex, France
** See annex of F. Romanelli et al, "Overview of JET Results", (24th IAEA Fusion Energy Conference, San Diego, USA (2012)).*

Preprint of Paper to be submitted for publication in Proceedings of the
21st International Conference on Plasma Surface Interactions, Kanazawa, Japan
26th May 2014 - 30th May 2014

ABSTRACT

Combining Lithium beam emission spectroscopy and edge reflectometry, localized Scrape-Off Layer (SOL) density modifications by Ion Cyclotron Range of Frequencies (ICRF) near fields were characterized in JET L-mode plasmas. When using the ICRF wave launchers connected magnetically to the Li-beam chord, the density decrease was steeper 2–3 centimetres outside the last closed flux surface (when mapped onto the outer mid-plane) and its value was halved at the outer limiters. The depletion depends on the ICRF power and on the phasing between adjacent radiating straps. Convection due to ponderomotive effects and/or $\mathbf{E}\times\mathbf{B_0}$ drifts is suspected. During ICRF-heated H-mode discharges in 2013, DC potentials up to 70V were measured locally over a few centimetres in the outer SOL by a floating reciprocating probe, located toroidally several metres from the active antennas. These observations are compared with probe measurements on ASDEX-Upgrade. Their implications for wave coupling, heat loads and impurity production are discussed.

1. MOTIVATIONS

Scrape-Off Layer (SOL) density conditions influence the way Ion Cyclotron Range of Frequency (ICRF) waves tunnel across the tenuous plasma periphery of magnetic fusion devices. This determines the ICRF power that can be transferred to the main plasma for a given Radio-Frequency (RF) current on the poloidal straps radiating the waves (or coupling resistance) [1, 2]. The far SOL density also affects the sputtering of impurities by the wall and the ICRF-induced heat loads on the antenna structures [3, 4]. Conversely the intense RF near fields in the vicinity of active ICRF antennas likely modify the SOL density. Such localized changes, indirectly suspected from a degradation of Lower Hybrid (LH) wave coupling [4,5, 6, 7], have been characterized more directly in most ICRF-heated machines, using probes [4, 8, 9], reflectometry [7] or active spectroscopy [10]. For the first time this paper undertakes a similar characterization at JET in L-mode, combining several types of diagnostics to investigate systematically 4-strap ICRF antennas. The challenges are to resolve the complex spatial structure of density modifications and to document their dependence with ICRF and plasma parameters. Their likely physical origin is also investigated, in light of reciprocating probe measurements during ICRF-heating on JET and ASDEX-Upgrade [9]. Possible consequences are finally discussed for ICRF and LH wave coupling, ICRF-specific impurity production and heat loads on ICRF antennas.

2. EXPERIMENTAL SETUP

On JET ICRF waves are excited by phased toroidal arrays of four straps [11] allowing launching waves with different spectra of wavevectors k_z in the toroidal direction. Dipole (phase difference [0, π, 0, π], main $k_z = 6.5\mathrm{m}^{-1}$) or Current Drive toroidal strap phasing (CD: [0,–π/2, –π, –3π/2], $k_z = 3.3\mathrm{m}^{-1}$) were used. Four such antennas are located toroidally around the JET vacuum chamber (see figure 1). Antennas C and D can be operated independently of the pair A+B, whose feeding transmission lines are coupled.

JET features two SOL density diagnostics, whose positions relative to the antennas are sketched on figure 1 for a typical pulse in the database. Lithium (Li) beam emission spectroscopy [12] probed the SOL along a vertical chord. For the edge safety factor $q_{95} = 3.8$, this observation volume crossed magnetic field lines passing in front of the top of antenna A and the middle of antenna B. The density distribution along this chord was subsequently mapped onto the outer mid-plane using reconstructed plasma equilibrium. A fast-sweeping X-mode edge reflectometer [13] measured the density distribution along a horizontal chord slightly above the outer mid-plane. It was connected magnetically to the bottom of antenna A and below antenna B. Both measurement volumes were located toroidally several meters away from the antennas. Within a radial shift by ±1cm the two diagnostics measured similar densities at the separatrix. Further outwards the profiles differed, partly because of the ICRF-specific effects investigated in this paper. However the density radial decay was generally slightly steeper with Li beam than with reflectometry, even in the ohmic regime. Using these diagnostics we investigated a database of L-mode plasmas heated in the [H]D minority scheme at frequency $f_0 = 42$MHz and magnetic field $B_0 = 2.4$-2.7T. This database included several parametric scans using each antenna independently during the first ICRF-heating experiments with the new JET ITER-Like Wall [14]. L-mode was also favored because ICRF-SOL interactions exist already in this regime and are easier to evidence in the absence of intermittent density disturbances due e.g. to Edge Localized Modes (ELMs).

3. LOCAL SOL DENSITY MODIFICATIONS DURING ICRF HEATING IN L-MODE.

Figure 2 shows the time-variations of the measured SOL density distributions over three successive ICRF pulses by the different antennas at similar power. The reflectometry measurements hardly evolved during ICRF application, within a fluctuating rigid radial shift by ±1cm. This trend is general to all the pulses analyzed. By contrast the Li beam profiles were modified in their outer part, within 20ms after ICRF switch-on and switch-off. The density modifications were specific to each antenna. Figure 3 details the density along the Li-beam chord, averaged over 0.8–1.2s-long time windows for the different phases in Figure 2. Colored regions around each profile represent the standard deviations of the density around their mean values. Within this uncertainty all the profiles agreed in their inner part. When unconnected antennas C or D were energized the density was quite similar to that in ohmic regime, nearly up to the radius where the observation point gets magnetically connected to the outer limiters of the machine (vertical dashed lines on figure 2). When the connected antenna pair A+B was powered, the measured profile decreased more steeply than the previous ones, at about 2cm outside the separatrix and 3cm in front of the outer limiters. The density at the leading edge of outer limiters reached half of its ohmic regime value. Outside this position all the profiles were different and their uncertainty was larger, but they all exhibited a reduced slope.

The differences between antennas and between diagnostics are mainly attributed to different magnetic connections of the probing chords to the active antennas. They suggest that the density becomes toroidally and poloidally inhomogeneous, and that the modifications can propagate

toroidally over several meters to the measurement locations. These geometrical properties are also inferred from LH wave coupling modifications [4][6]. Density measurements combined with antenna toggling similar to figure 2 were repeated during a dynamic scan of the edge safety factor between $q_{95}=4.2$ and $q_{95}=3.2$. The density decrease along Li-beam chord was steeper at higher $q_{95,}$ both in the ohmic and ICRF-heated phases. However the measured Li-beam profiles with antenna pair A+B always exhibited a density depletion compared to those in the ohmic regime at similar q_{95}. Over the scan the altitude of the magnetic connection from the Li-beam to a reference poloidal cross-section at the middle of antenna B varied from Z=+40cm to Z=-15cm at the radius of maximal depletion. This provides a lower bound for the poloidal extent of the ICRF-perturbed zone.

Figure 4 shows that the radial steepening of the Li beam profiles 2cm outside the separatrix, already present for 0.5MW distributed over 8 straps in CD phasing, was gradually enhanced with higher power, with a possible saturation. Power coupling depends on the ICRF Fast wave peripheral evanescence below a typical cut-off density of $5\times10^{17}\mathrm{m}^{-3}$ for $k_z=3.3\mathrm{m}^{-1}$ [2]. In figure 4 this cutoff layer moved radially by δR_{cutoff}~1cm over the covered power range. Assuming that a similar δR_{cutoff} occurs in front of the straps, an upper bound for the associated modification of wave evanescence factor is $k_z\delta R_{cutoff}$~0.03<<1. Consistently with this modest change, that could besides be poloidally localized, the measured ICRF coupling resistance did not vary significantly over the covered RF power range (see inset). Similar behavior was obtained in dipole phasing. For equivalent RF power the density decrease was smaller than with CD phasing.

4. INTERPRETATION AND COMPLEMENTARY PROBE MEASUREMENTS.

The spatial localization of the measured density variations on outer flux tubes, their fast response to ICRF wave application, their parametric dependence with local RF power and strap phasing, point to a non-linear effect associated with the near RF fields close to the active antennas. Ponderomotive density expulsion is expected in the region where these near RF fields are intense [15]. Yet these local perturbations need to propagate toroidally up to the diagnostic chords, where the expected local RF field amplitude is modest. This propagation could be caused by DC flows, associated with the inhomogeneous ponderomotive effects in magneto-active plasmas [15]. The magnitude of these flows remains to be quantified.

Alternatively the intense near RF fields could interact with the sheaths at the extremities of open field lines and cause a DC biasing of the antenna environment that can easily propagate toroidally [8, 16]. Sheath rectification is indirectly suspected from an ICRF-specific impurity production in the JET vacuum chamber [14, 17] and RF-induced heat loads on active antennas [3]. More direct hints of local plasma biasing are provided by reciprocating probe measurements during ICRF-heated H-mode plasmas in 2013. A Langmuir probe was installed on a reciprocating mount in a vertical port. Its vertical trajectory was connected magnetically to several outer limiters between antenna D and antenna A (i.e. at different location than the Li beam, see figure 1). Figure 5 plots along the probe trajectory the DC potential recorded by a floating electrode between ELMs and time-averaged

over fluctuations. During ICRF a localized peak was recorded for magnetic connections near the leading edge of the outer limiters. Its amplitude was 70V for 3MW total ICRF power coupled by all four antennas, decreased below 40V for 1MW and was absent in a NBI-only discharge. Peaks of both signs were recorded depending on the pulse. Towards the wall the peak radial extent was 1–2cm at outer mid-plane. The probe could unfortunately plunge no further than 5mm in front of the outer limiters. It was neither possible to determine which antenna was responsible for the peak. Although the probe floating potential is not the plasma potential, SOL biasing is suspected, with large radial inhomogeneity. The associated $\mathbf{E}\times\mathbf{B_0}$ convection could modify the density in the outer SOL [8, 16].

This interpretation is complemented by Retarding Field Analyser (RFA) measurements in L-mode on ASDEX-Upgrade. These were detailed in reference [9] and are briefly summarized here. A reciprocating RFA measured two quantities in both directions along magnetic field lines: the ion saturation current I_{slit} on the entrance slit plates, proportional to the ion influx and the mean parallel energy $<W_{//}>_t$ of collected ions, averaged over many RF periods. Combining multiple RFA reciprocations over a scan of q_{95} provided 2D poloidal/radial resolution. A localized RF-perturbed zone was evidenced on the RFA side magnetically connected to an active ICRF antenna, several metres away toroidally from the wave launcher. Figure 6 shows a flat 2D I_{slit} pattern surrounded by steep gradients. Correlatively $<W_{//}>_t$ exceeding 160eV was observed locally at the same place, while it remained below 40eV in the unperturbed zone. The center of the ICRF-modified zone is connected radially slightly behind the leading edge of antenna side limiters. The zone is broadest (radial extension up to 5cm) and $<W_{//}>_t$ is largest near the bottom of the active antenna. The local ion acceleration is interpreted as due to local biasing. The spatially inhomogeneous bias could generate $\mathbf{E}\times\mathbf{B_0}$ flows around the flat I_{slit} zone. In addition to the resulting local density depletion, the plasma biasing could diminish the slit plate effective collection area and contribute to reduce I_{slit}.

5. DISCUSSION AND OUTLOOK

Density changes were evidenced experimentally in the outer SOL during ICRF heating on JET. Their complex 3-dimensional spatial pattern could not be fully characterized. But the observed changes appeared mainly on magnetic field lines passing in front of active ICRF antennas and/or connected magnetically to the outer limiters, implying toroidal, poloidal and radial localization. Parametric dependence with local ICRF power and strap phasing was outlined. Probe measurements suggest a local biasing in the outer SOL during ICRF heating. Both potential and density modifications propagate several meters away from the active antennas in the parallel direction, but their value at the measurement location could differ from that in front of the straps.

Convection from ponderomotive effects and/or $\mathbf{E}\times\mathbf{B_0}$ drifts was invoked to explain the observed density changes. The two mechanisms do not exclude each other. At least one process involves plasma biasing, that is also suspected for enhanced sputtering. In that case the location of the density changes might provide hints about ICRF-specific sources of tungsten in the main chamber of JET

with the ITER-like wall, that have not been clearly identified yet [14]. The spatial pattern of the modification also puts strong constraints on numerical simulations [15, 18] and on antenna design optimization.

Both RF measurements and observed density changes suggest that the local SOL modifications do not significantly alter the ICRF wave coupling on JET. LH wave coupling was more strongly affected. For efficient combined operation the near-field-induced local density depletion was partly compensated with a localized gas fuelling close to the LH wave launchers [5]. A similar technique is being developed for improving ICRF wave coupling without degrading the overall plasma performance [1, 2]. It is not clear how these different physical processes could interfere, e.g. how a local convective transport in front of the antennas might redistribute a poloidally localized source of particles. This interaction needs to be accounted for when designing a dedicated gas injection valve for ICRF antennas in ITER. Density convection might also redistribute the ICRF-specific heat loads poloidally on the antenna structure [4]. Monitoring the local SOL density therefore becomes important for physical understanding and operational optimization, using if possible dedicated diagnostics directly embedded in the antennas [7, 10, 19, 20].

ACKNOWLEDGEMENTS

This work, supported by the European Communities under the contract of Association between EURATOM and CEA, was carried out within the framework of the European Fusion Development Agreement. The views and opinions expressed herein do not necessarily reflect those of the European Commission or of the ITER Organization.

REFERENCES

[1]. P. Jacquet et al., *Nuclear Fusion* **52** (2012) 042002 (6pp)

[2]. E. Lerche et al., "Impact of gas injection on ICRF coupling and SOL parameters in JET-ILW H-mode plasmas", this conference, paper P1.061

[3]. P. Jacquet et al., *Journal of Nuclear Materials* **438** (2013) p. S379–S383

[4]. L. Colas et al., *Plasma Physics and Controlled Fusion* **49** (2007) pp. B35–B45

[5]. A. Ekedahl et al., AIP Conf. Proc. **694** p. 259–62 (2003)

[6]. K. Kirov at al., *Plasma Physics and Controlled Fusion* **51** (2009) 044003 (20pp)

[7]. C. Lau et al., *Plasma Physics and Controlled Fusion* **55** (2013) 095003 (13pp)

[8]. Bécoulet M. et al., *Physics of Plasmas* **9** (2002) p.2619

[9]. L. Colas et al., *AIP conf. Proceedings* **1580**, p.259-262 (2014)

[10]. K. Crombé et al., Proc. 40th EPS conf. on plasma phys. Contr. Fusion Espoo (Finland) 2013 ECA vol **37D** P4.184

[11]. A. Kaye et al., SOFE Conf. Proc., 16th IEEE/NPSS Symposium, Vol. 1 p736 (1995)

[12]. M. Brix, et al., *Review of Scientific Instruments*, **81** (2010), 10D734

[13]. A. Sirinelli, et al., *Review of Scientific Instruments*, **81** (2010), 10D939

[14]. V. Bobkov et al., *Journal of Nuclear Materials* **438** (2013) S160–S165
[15]. D. Van Eester et al. *Plasma Physics and Controlled Fusion* **55** 025002 (2013)
[16]. D.A. D'Ippolito, J.R. Myra, J. Jacquinot, M. Bures, *Physics of Fluids* **B5** (10), 1993, p. 3603
[17]. C.C. Klepper et al., *Journal of Nuclear Materials* **438** (2013) S594–S598
[18]. J. Jacquot et al., *AIP Conf. Proc.* **1580**, 97 (2014), Submitted to *Physics of Plasmas* 2014
[19]. F. Clairet et al., "Reflectometry diagnostic for density measurements in front of the ITER ICRH antenna", proc. 11th International Reflectometry Workshop, Palaiseau 22-24 April 2013
[20]. O. Tudisco et al. *AIP conf. Proceedings* **1580**, pp.566-569 (2014)

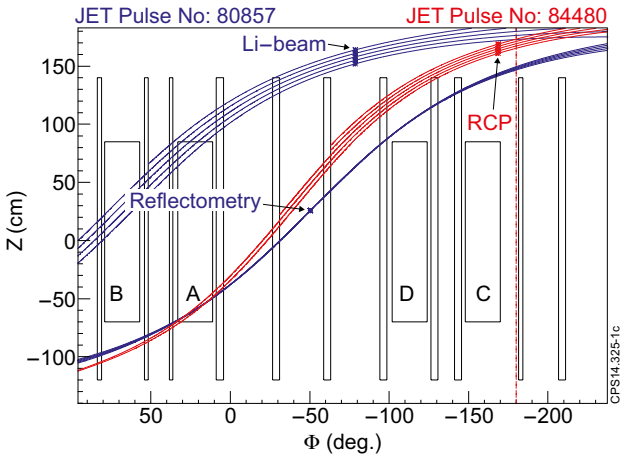

Figure 1: Toroidal/vertical sketch of ICRF antennas and outer limiters in JET, as seen from inside the vacuum vessel. Magnetic field line tracing from several points along Lithium beam and reflectometry chord on pulse JET Pulse No: 80857 (blue) and reciprocating probe trajectory on pulse JET Pulse No: 84480 (red).

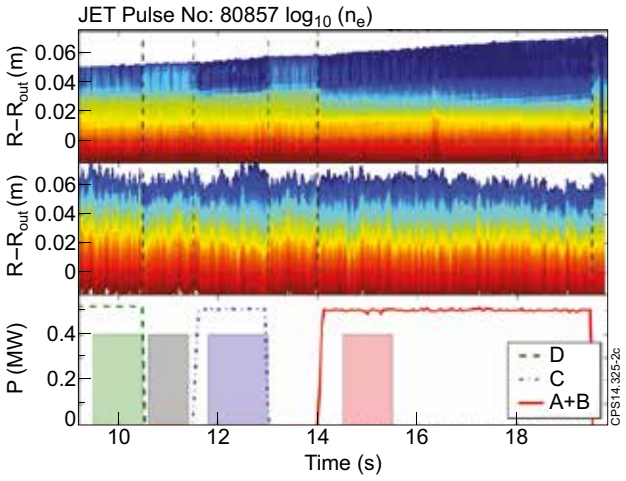

Figure 2: Time traces during JET Pulse No: 80857. Top panel: density (logarithmic scale) along Li beam chord versus time and radial distance to separatrix (horizontal dashed line) in outer mid-plane. Color scale between 2×10^{17} m^{-3} and 1×10^{19} m^{-3}. Middle: same for reflectometry measurements, same color scale. Bottom: RF power delivered by the different ICRF antennas with CD phasing, and time windows for averaging the profiles on figure 3.

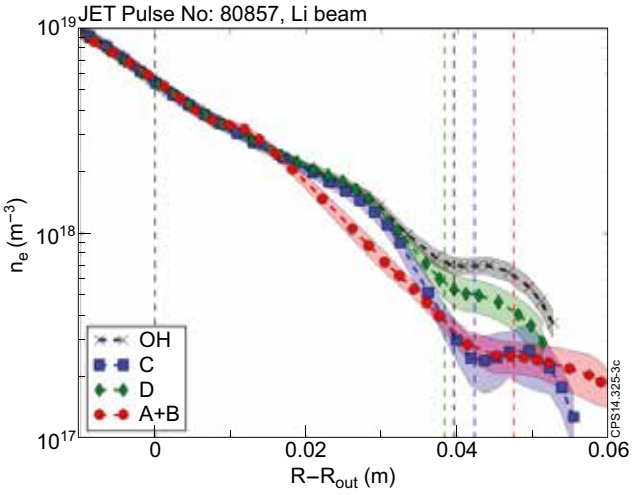

Figure 3: Li beam density profiles averaged over the four time windows in figure 2, versus distance to separatrix in outer mid-plane. Colored regions: standard deviation of n_e around its averaged value. Colored dashed lines: Li beam magnetically connected to outer limiter.

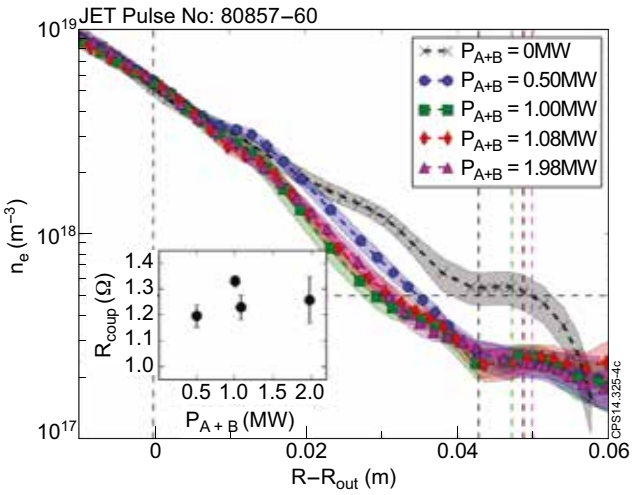

Figure 4: Time-averaged Li-beam density profiles over ICRF power scan by A+B pair in CD strap phasing, versus distance to separatrix in outer mid-plane. Horizontal dashed line: characteristic cut-off density for main $k_z = 3.3m^{-1}$ in radiated spectrum for CD phasing. Inset: coupling resistance averaged over antenna pair A+B, versus coupled power.

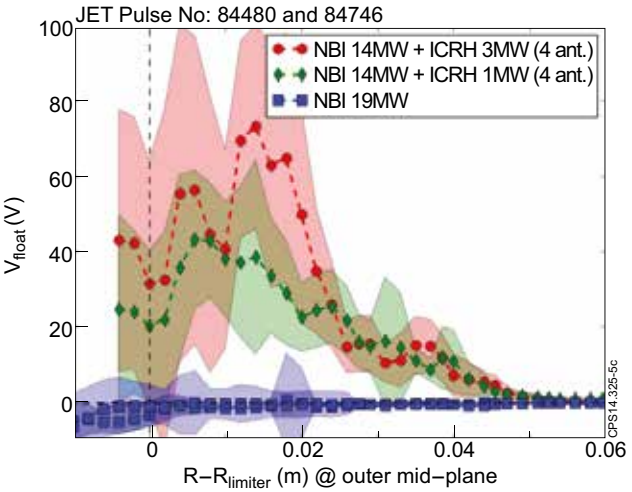

Figure 5: Floating potential of reciprocating probe, time averaged between ELMs, versus radial distance to leading edge of outer limiters at the outer mid-plane. Colored regions: standard deviation around mean value. Vertical dashed line: leading edge of outer limiter.

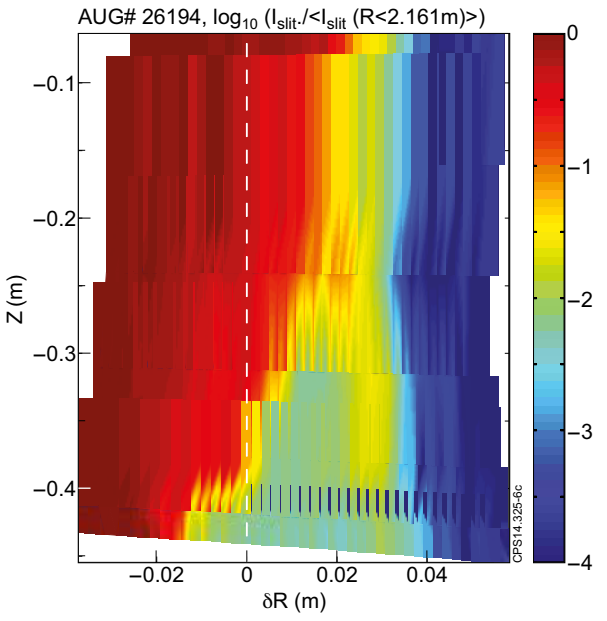

Figure 6: Current collected on saturated RFA slit plate (log. scale) normalized to its value two centimetres in front of antenna limiter, versus coordinates (δR,Z) of the connection point from the probe to an ICRF antenna delivering 600kW on ASDEX-Upgrade. A curved coordinate system was used, where dR represents the radial distance to the leading edge of the antenna side limiter (dashed vertical line δR = 0). Separatrix was at δR = –6.5cm.